Hysteresis Relation between Turbulence and Temperature Modulation during the Heat Pulse Propagation into a Magnetic Island in DIII-D

K. Ida, T. Kobayashi, M. Ono, T. E. Evans, G. R. McKee, and M. E. Austin

Hysteresis relation between turbulence and temperature modulation during the heat pulse propagation into a magnetic island in DIII-D

K. Ida,[1,2] T. Kobayashi,[1,2] M. Ono,[3] T.E. Evans,[4] G.R. McKee,[5] and M.E. Austin[6]

[1]National Institute for Fusion Science, National Institutes of Natural Sciences, Toki, Gifu 509-5292, Japan
[2]SOKENDAI (The Graduate University for Advanced Studies), Toki, Gifu 509-5292, Japan
[3]National Institutes for Quantum and Radiological Science and Technology, Naka, Ibaragi, 311-0193, Japan.
[4]General Atomics, San Diego, California 92186-5608, USA
[5]University of Wisconsin-Madison, Madison, Wisconsin 53706, USA
[6]University of Texas, Austin, Texas 78712, USA
(Dated: May 14, 2018)

The hysteresis relation between turbulence and temperature modulation during the heat pulse propagation into a magnetic island is studied for the first time in toroidal plasmas. Lissajous curves of the density fluctuation ($\tilde{n}/n$) and the electron temperature (T_e) modulation show that the ($\tilde{n}/n$) propagation is faster than the heat pulse propagation near the O-point of the magnetic island. This faster $\tilde{n}/n$ propagation is an experimental evidence of the turbulence spreading from X-point to the O-point of the magnetic island.

PACS numbers: 52.55.Fa, 52.35.Ra, 52.35.Py

Magnetic islands are widely observed in both laboratory plasma and astrophysical plasma. The turbulence inside the magnetic island is an important issue because it has a significant impact on transport characteristics in toroidal plasmas and turbulent reconnection of magnetic field in the solar flare [1, 2]. Therefore, the study of the hysteresis relation between the turbulence level and the perturbation of the plasma parameter such as temperature is essential for understanding the dynamics and mechanism driving plasma turbulence. The hysteresis relation between the turbulence level and the radial electric field has been studied in laboratory plasmas using limit-cycle oscillation with the frequency of 2-5 kHz and the phase delay between the turbulence and the radial electric field is observed in the turbulence time-scale [3, 4]. Magnetic islands define a unique region in the plasma because there are no temperature and density gradients, which drive the turbulence. Since the heat propagation inside the magnetic island is relatively slow [5, 6], turbulence could propagate faster than the heat pulse, if there is a turbulence spreading [7] from X-point (or boundary) to the O-point of the magnetic island. If the turbulence level is simply determined by the local temperature gradients or local radial electric field, the propagation of the turbulence should track to the propagation of heat pulse within a turbulence time scale ($< 10^{-4}$ sec) because the propagation of the heat pulse has a time scale of $10^{-3} \sim 10^{-2}$ sec. Therefore, the study of the dynamic linkage (hysteresis relation) between the turbulence level and temperature modulated inside the magnetic island provides new and important information for the turbulence spreading and a new research area of non-local interaction between electron temperature (T_e) changes and density fluctuation ($\tilde{n}$). However, this hysteresis relation has not been studied previously, in spite of its importance. In this letter, we show the hysteresis relation between the $\tilde{n}/n$ and the T_e modulation during the heat pulse propagation into a magnetic island in DIII-D in order to clarify the dynamic relation between the $\tilde{n}/n$ and the T_e modulation inside the magnetic island.

For purposes of obtaining a better understanding of fluctuation-driven transport inside a magnetic island, repetitive heat pulses were injected into a magnetic island in the DIII-D tokamak. DIII-D is a tokamak device with D-shape poloidal cross section, a major radius of 1.7 m, and minor radius of 0.6 m for magnetic confinement of high temperature plasmas. In this experiment, the plasma current was 1.28 MA and the toroidal magnetic field was 1.92 T with an inner wall limiter configuration and a edge safety factor of $q_{edge} = 4.5$ ($q_{95} = 3.8$). The electron density (n_e) was 3.9-4.6 $\times 10^{19}\,\mathrm{m}^{-3}$ and the T_e in the core region was 2.0-2.1 keV. RMP fields produced by a non-axisymmetric magnetic field perturbation coil (C-coil) are used to produce magnetic islands at the resonant surface [12]. In this experiment, the perturbation field has a resonance at a safety factor of $q = 2$ and the poloidal and toroidal mode numbers (m, n) are (2,1). The location of the magnetic island can be rotated toroidally by 180° by changing the toroidal phase ($\phi_{n=1}$) of C-coil from $\phi_{n=1} = 5°$ to $\phi_{n=1} = 185°$ or vice versa (phase flip). As a result of this phase flip, the X-point and O-point of the magnetic island appears between the electron cyclotron emission (ECE) measurement for T_e at $\phi = 81°$ and at the beam emission spectroscopy (BES) measurement for $\tilde{n}$ at $\phi = 150°$. The electron cyclotron heating (ECH) power is deposited at $\rho=0.42$ with a modulation frequency of 50 Hz and it heats the electrons and modifies T_e. Here, normalized minor radius $\rho = \sqrt{\psi_N}$ where ψ_N s a normalized toroidal flux, such that it is 0 on the magnetic axis and 1 at the Last Closed Flux Surface (LCFS).

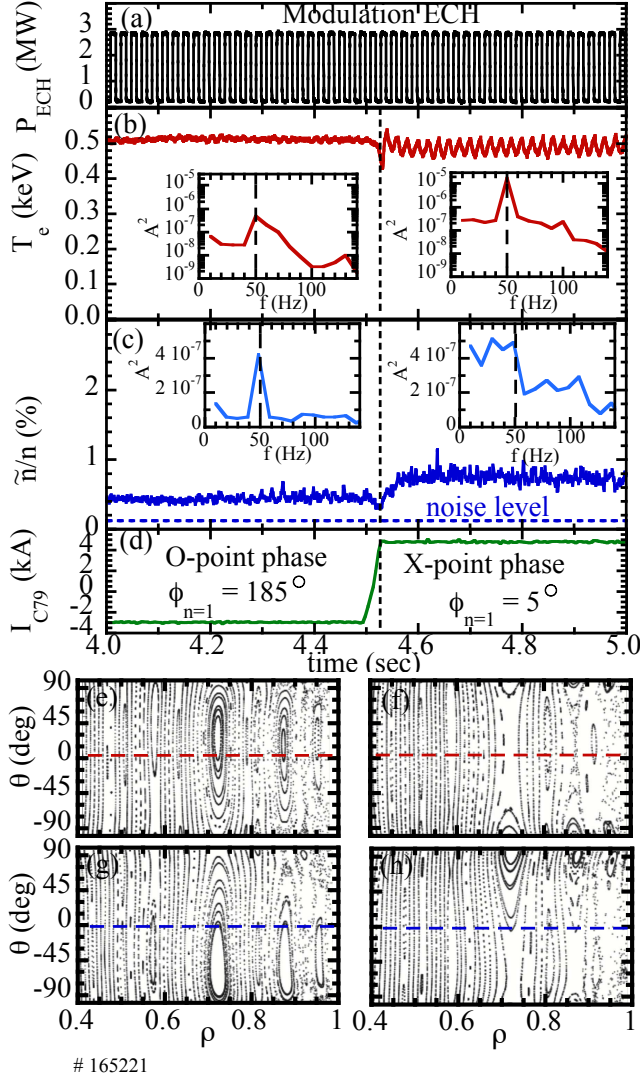Figure 1 shows the time evolution of ECH power,

FIG. 1: Time evolution of (a) power of ECH, P_{ECH} (b) T_e measured with the ECE at $\rho = 0.74$, (c) $\tilde{n}/n$ integrated from 10 kHz to 50 kHz at $\rho = 0.74$, and (d) current of C-coil and Poincaré map at the poloidal cross section of T_e measurements in (e) O-point and (f) X-point phase and Poincaré map at the poloidal cross section of $\tilde{n}/n$ measurements in (g) O-point and (h) X-point phase. The frequency spectrum of T_e modulation and envelop of density fluctuation are also plotted in Figure (b) and (c).

P_{ECH}, T_e measured with ECE at $\rho = 0.74$, $\tilde{n}/n$ measured with BES at $\rho = 0.74$ near the O-point or the X-point of the magnetic island, and the current of one of the C-coils of C79. Here, $\tilde{n}$ is the envelop of density fluctuation integrated in the frequency range of 10 - 50 kHz. The sign flip of the current in C79 seen in figure 1 (d) indicates the flip of phase of $n = 1$ perturbation with the toroidal angle of 185° and 5°. In this paper, the period with perturbation field of 185° and 5° is called O-point phase and X-point

phase, respectively. The Poincaré map at the poloidal cross section of the T_e and the $\tilde{n}/n$ measurements in the O-point phase and the X-point phase are also plotted, where the x-axis is the normalized minor radius (ρ) and the y-axis is the poloidal angle (θ). The Poincaré map shows the 3D vacuum perturbation field from the C-coil superimposed on the axisymmetric DIII-D equilibrium field reconstructed using the EFIT code. The perturbation field of the C-coils has various Fourier components $\delta B(m, n)$ that have a resonance at $q = 2, 3, 4$. Here, the perturbation fields are calculated using the Fourier analysis module in the trip3d code [12]. There is no $q = 1$ rational surface because the $q_{\min} > 1$ in this plasma. The $n = 1$ poloidal mode strength for this shot is 8.1, 7.7, 7.4 gauss for the poloidal mode number of $m = 2, 3, 4$, respectively. There are also high-n modes produced but these are more than an order of magnitude smaller than the $n = 1$ modes. The $m/n = 2/1, 3/1$ and $4/1$ magnetic islands appear at the normalized minor radius ρ of 0.74, 0.88, and 0.96, respectively. In this experiment, the width of the 2/1 magnetic island is enlarged compared to the vacuum islands seen in figure 1(e-h). At the O-point phase, the poloidal angle of O-point, $\theta_O = +20°$ (the poloidal angle of X-point, $\theta_X = -110°, +110°$) for T_e measurements and $\theta_O = -40°$ ($\theta_X = -130°, +110°$) for $\tilde{n}/n$ measurements. At the X-point phase, $\theta_X = +20°$ ($\theta_O = -110°, +110°$) for T_e measurements and $\theta_X = -40°$ ($\theta_O = -130°, +90°$) for $\tilde{n}/n$ measurements. As seen in figure 1(a), the modulation frequency of ECH power is set to 50 Hz, which is low enough to investigate the slow heat pulse propagation inside the magnetic island. The modulation amplitude of T_e in the O-point phase ($t < 4.52$ sec), where the O-point of the magnetic island is located near the poloidal cross section of the T_e and the $\tilde{n}/n$ measurements, is much smaller than that in the X-point phase ($t > 4.52$ sec). Here, the X-point of the magnetic island is located near the poloidal cross section of the T_e and the $\tilde{n}/n$ measurements. The $\tilde{n}/n$ level is also lower in the O-point phase than that in the X-point phase. The frequency spectrum of T_e modulation and envelope of density fluctuation is also plotted in Figure.1. It is interesting that the frequency spectrum of T_e modulation shows narrower peak at the modulation frequency (50Hz) with X-point, while the envelope of density fluctuation shows narrower peak at the O-point of the magnetic island. This observation shows a strong correlation between the T_e modulation at the X-point and the density fluctuation at the O-point of the magnetic island.

In order to improve the signal to noise ratio, we perform a conditional average of ECE and BES signal as function of relative time of τ. This is defined as $(1/N)\Sigma_{i=1}^{N}\Psi(t_i + \tau)$, for an arbitrary variable Ψ, where t_i indicates the i-th time of MECH turn-on and N is the number of modulation. Figure 2 shows the patterns of conditionally sampled signals, radial profiles of mean T_e, amplitude and delay time of T_e modulation, $\tilde{n}/n$ levels,
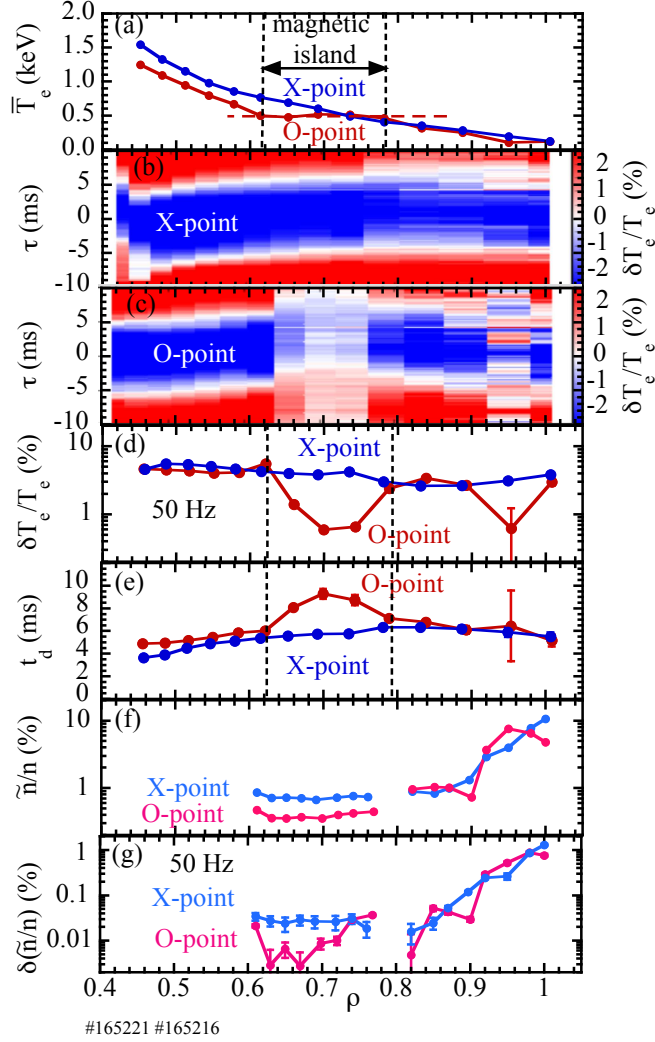
FIG. 2: Radial profiles of (a) mean T_e, the patterns of conditionally sampled signals in (b) X-point and (c) O-point phase, (d) normalized T_e modulation amplitude, $\delta T_e/T_e$, (e) delay time of T_e modulation (t_d) given by the phase shift between ECH pulse and T_e modulation, (f) $\tilde{n}/n$ levels measured with BES, and (g) $\tilde{n}/n$ modulation amplitude, $\delta(\tilde{n}/n)$ levels, in the O-point phase and X-point phase.

and modulation amplitude of $\tilde{n}/n$ in the O-point phase and the X-point phase. The modulation amplitude is defined from coefficient of Fourier component of ECE and BES signal at the frequency of ECH modulation (50 Hz). The T_e profile shows the flattening at $\rho = 0.62$-0.77 in the O-point phase, while there is no T_e flattening observed in the X-point phase. As seen in figure 2(d), the modulation amplitude of T_e inside the magnetic island (O-point) is much smaller than that outside the magnetic island by a factor of $5 \sim 6$. This is in contrast to no reduction of modulation amplitude of T_e at the X-point of the magnetic island. The reduction of modula-

tion amplitude is due to the slow heat pulse propagation inside the magnetic island as observed in the peaked t_d inside the magnetic island in figure 2(e). The peaked t_d indicates that the heat pulse induced by the modulated ECH power propagates faster across the X-point and then slowly propagates towards the O-point of the magnetic island. Heat pulse propagation speed inside the magnetic island is much slower than the speed outside the magnetic island and at the X-point. The delay time increases monotonically in the X-point but not in the outer region ($\rho > 0.8$) during the O-point phase as seen in Figure 2(b)(c)(d)(e). This is due to the effect of the higher harmonics components of the heat pulse, which have a faster speed and longer decay length than that predicted by a diffusive model [8] Therefore, a simple heat pulse propagation analysis with a fundamental component only gives an apparent roll over of the delay time especially near the plasma edge, where the effect of higher harmonics component becomes relatively large particularly in the O-point phase.

As seen in figure 2(f), the magnitude of the $\tilde{n}/n$ measured with the BES shows a sharp decrease in the plasma core from the plasma edge. The magnitude of the $\tilde{n}/n$ at the O-point is smaller than that at the X-point by a factor of $2 \sim 3$, while the magnitude of the $\tilde{n}/n$ outside magnetic island region ($\rho = 0.82$-1.0) is almost identical between the O-point phase and the X-point phase. These results are consistent with the previous results observed in the Doppler back scattering (DBS) [9, 10] and a significant reduction of thermal diffusivity inside the magnetic island observed in JT-60U [11]. The lower level of the $\tilde{n}/n$ in the O-point seen in Figure 2(f) results in the reduction of transport, which is consistent with the slower heat pulse propagation as seen in Figure 2(e). The modulation amplitude of the $\tilde{n}/n$ is also reduced inside the magnetic island as seen in figure 2(g). The small modulation amplitude of $\tilde{n}/n$ is attributed to the small modulation amplitude of T_e. The difference in the width of the magnetic island between the T_e measurements and the $\tilde{n}/n$ measurements is due to the difference in toroidal angle between the two diagnostics as seen in figure 1 (e) and (g). The reduction of $\tilde{n}/n$ level is observed in the entire region near the magnetic island at the O-point as seen in figure 2(f). In contrast, as seen in figure 2(g), the reduction of the 50 Hz modulation amplitude of $\tilde{n}/n$ driven by the T_e modulation is observed deep inside the magnetic island where the T_e modulation is significantly reduced. This wider width of the reduced $\tilde{n}/n$ observed in this experiment is interpreted as the reduction of $\tilde{n}/n$ due to the flow shear that often appears at the boundary of the magnetic island [13]. The small drop of the fluctuation and the modulation amplitude at $\rho \sim 0.9$ implies the existence of m/n=3/1 magnetic island.

The hysteresis relation between the $\tilde{n}/n$ and T_e modulation is investigated in order to study the causal relation between the propagation of the $\tilde{n}/n$ and the heat pulse.
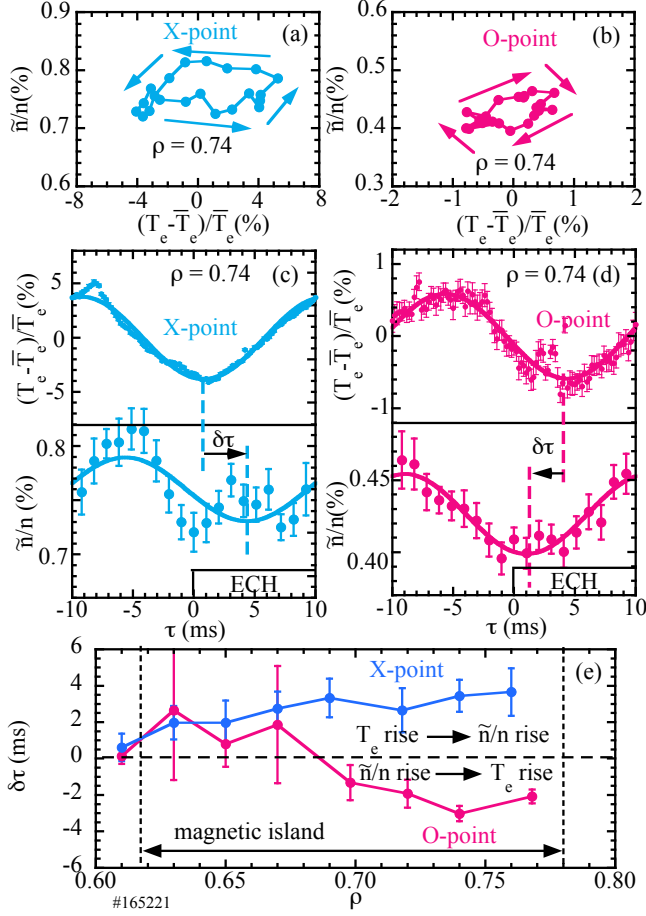
FIG. 3: Hysteresis of amplitude between $\tilde{n}/n$ and T_e modulation at $\rho = 0.74$ in the (a) X-point and (b) O-point, time evolution of T_e and $\tilde{n}/n$ at $\rho = 0.74$ in the (c) X-point and (d) O-point phase with the relative time (τ) respect to the onset of ECH, and (e) radial profiles of delay time difference between modulation of T_e and $\tilde{n}/n$ ($\delta\tau$) at X-point phase and the O-point phase.

The T_e profile inside the magnetic island is modulated between slightly peaked and slightly hollow by the heat pulse propagation. However, the T_e is expected to be isothermal on magnetic flux surface and the T_e gradient at the O-point is also expected to be zero because of the topology of the magnetic island. Therefore, the hysteresis relation between local turbulence and local T_e is discussed rather than the relationship between the turbulence and the T_e gradient, which is not a good measure of hysteresis in a magnetic island. Figure 3 shows the results of conditional average sampled aforementioned. As seen in figure 3 (a) and (b), there is a clear difference in the hysteresis relation between the O-point and the X-point. In the X-point, the hysteresis relation shows counter clockwise (CCW) direction, while it shows clockwise (CW) direction in the O-point. These results show

that the change in T_e precedes the change in $\tilde{n}/n$ in the X-point, while the change in $\tilde{n}/n$ precedes the change in T_e at the O-point.

The delay time difference between modulation of T_e and $\tilde{n}/n$ ($\delta\tau$) is evaluated from the phase delay of sinusoidal wave function which gives the best fit to the measurements. As seen in figure 3 (c) and (d), the $\delta\tau$ is $2 \sim 3$ ms at the X-point, while this $\delta\tau$ becomes negative ($-2 \sim -3$ ms) at $\rho = 0.74$ at the O-point. It should be noted that density fluctuations in the X-point region exhibit higher harmonic oscillations, while there is little higher harmonic oscillation in the density fluctuation in O-point, which is also shown in figure 1(c). Radial profiles of $\delta\tau$ at the X-point and the O-point are plotted in figure 3 (e). The $\delta\tau$ is positive in the entire region at the X-point, which indicates that the fluctuation responds to the change in the T_e gradient due to the heat pulse propagation. The T_e gradient across the x-point is larger than the one across the O-point as shown in figure 2(a), which causes the thermal transport to lead the change in the $\tilde{n}/n$ resulting in the positive (CCW) hysteresis. This result is consistent with the previous result that the $\tilde{n}/n$ level increases as the T_e gradient is increased [10]. However, the $\delta\tau$ in the O-point is positive in the inner region ($\rho < 0.68$) and negative in the outer region ($\rho > 0.68$). The negative $\delta\tau$ observed shows that the propagation of fluctuation is faster than that of the heat pulse, which is similar to the observation in LHD [14].

The positive and negative $\delta\tau$ observed in this experiment imply the existence of the non-locality of the transport, because the existence of hysteresis is evidence of non-locality in the transport [15, 16]. The negative $\delta\tau$ is associated with the CW hysteresis in the O-point due to the $\tilde{n}/n$ leading the heat pulse in the island O-point. A possible physics model here is that the heat pulse is shunted in the parallel direction around the good internal island flux surfaces while the perpendicular thermal transport into the island O-point is slow, as seen in figure 2(c) and can only be enhanced once the $\tilde{n}/n$ increase sufficiently to enhance the cross-field thermal transport. On the other hand, the thermal transport at the x-point is enhanced by the stochastic field lines which allows the fast parallel thermal transport to lead the $\tilde{n}/n$ across that region of the island compared to the O-point. The negative $\delta\tau$ indicates that the fluctuation propagates from the X-point of the magnetic island by turbulence spreading before the heat pulse propagates into the O-point of the magnetic island.

The enhancement of heat pulse propagation speed due to the turbulence spreading could be one of the candidates to explain the bifurcation between high-accessibility state (with larger amplitude and fast heat pulse propagation) and low-accessibility state (with smaller amplitude and slower heat pulse propagation) of the O-point of the magnetic island [17]. In the high-accessibility state, the $\tilde{n}$ penetrates into the O-point

across the x-point by turbulence spreading and leads the enhancement of transport and heat pulse propagation. Turbulence spreading can be shielded by the radial electric field shear (E_r) shear [18] which is localized at the boundary of the stationary magnetic island [11, 13, 19]. Therefore, if the E_r shear becomes large enough to shield the turbulence spreading, the $\tilde{n}$ does not penetrate into the O-point of the magnetic island and results in the reduction of transport and slow heat pulse propagation inside the magnetic island as seen in the low-accessibility state. Once the turbulence spreading is shielded, the E_r shear is expected to increases due to the reduction of viscosity. Then the bifurcation between the following two states are possible; one is weak turbulence spreading with the large E_r shear and the other is strong turbulence spreading with the small E_r shear. The slight change in E_r field shear at the boundary of the magnetic island can cause the bifurcation between high-accessibility and low-accessibility state.

In conclusion, the hysteresis relation between the turbulence and the T_e modulation during the heat pulse propagation into a magnetic island is studied in DIII-D. The $\delta\tau$ is negative (fluctuation propagation is faster than the heat pulse propagation) in the low field side of the O-point inside the magnetic island, while it is positive (fluctuation propagation is slower than the heat pulse propagation) in the entire region near the X-point of magnetic island. The observations of hysteresis and the large difference in delay time between the propagation of fluctuation and heat pulse suggests the feedback loop between the turbulence propagation and heat pulse propagation, where the faster propagation of turbulence enhances the speed of the heat pulse propagation. Understanding transport inside magnetic islands should have a strong impact on the prediction of the H-mode threshold power in ITER, where the resonant magnetic perturbations (RMPs) is applied recognized to suppress the edge localized mode (ELM) in order to avoid damage to the wall due to the transient heat load to the divertor in tokamaks [20, 21].

[1] K. Shibata and S. Tanuma *Earth Plants Space* **53**, 473 (2001).
[2] N. Nishizuka and K. Shibata, *Phys. Rev. Lett.* **110**, 051101 (2013).
[3] J. Cheng, *et. al.*, *Phys. Rev. Lett.* **110**, 265002 (2013).
[4] T. Kobayashi, *et. al.*, *Phys. Rev. Lett.* **110**, 035002 (2013).
[5] S. Inagaki, *et. al.*, *Phys. Rev. Lett.* **92**, 055002 (2004).
[6] L. Bardóczi, *et. al.*, *Phys. Plasmas* **24**, 062503 (2017).
[7] T. S. Hahm, *et. al.*, *Plasma Phys. Control. Fusion.* **46**, A323 (2004).
[8] T. Kobayashi, *et. al.*, *Nucl. Fusion* **57**, 076013 (2017).
[9] L. Bardóczi, *et. al.*, *Phys. Plasmas* **23** 052507 (2016).
[10] L. Bardóczi, *et. al.*, *Phys. Plasmas* **24**, 056106 (2017).
[11] K. Ida, *et. al.*, *Phys. Rev. Lett.* **109**, 065001 (2012).
[12] T. E. Evans, R. A. Moyer and P. Monat, *Phys. Plasmas* **9** 4957 (2002) .
[13] K. Ida, *et. al.*, *Phys. Rev. Lett.* **88**, 015002 (2001).
[14] S. Inagaki, *et. al.*, *Nucl. Fusion* **53** 113006 (2013).
[15] K. Ida, *et. al.*, *Nucl. Fusion* **55**, 013022 (2015).
[16] K. Itoh, *et. al.*, *Nucl. Fusion* **57**, 102021 (2017).
[17] K. Ida, T. Kobayashi, T. E. Evans, *et. al.*, *Sci. Rep.* **5**, 16165 (2015).
[18] W. X. Wang, *et. al.*, *Phys. Plasmas* **14**, 072306 (2007).
[19] A. B. Navarro, *et. al.*, *Plasma Phys. Control. Fusion.* **59**, 034004 (2017).
[20] T. E. Evans, *et al Nature Phys.* **2**, 419 (2006).
[21] Y. Liang, *et. al.*, *Phys. Rev. Lett.* **98**, 265004 (2007).